First-principles calculations of the atomic and electronic structure of $SrZrO_3$ and $PbZrO_3$ (001) and (011) surfaces

2010 J. Phys.: Condens. Matter 22 415901

(http://iopscience.iop.org/0953-8984/22/41/415901)

J. Phys.: Condens. Matter **22** (2010) 415901 (10pp) doi:10.1088/0953-8984/22/41/415901

First-principles calculations of the atomic and electronic structure of $SrZrO_3$ and $PbZrO_3$ (001) and (011) surfaces

R I Eglitis[1] **and M Rohlfing**[2]

[1] Institute of Solid State Physics, University of Latvia, 8 Kengaraga Street, Riga LV1063, Latvia
[2] Universität Osnabrück, Fachbereich Physik, D-49069 Osnabrück, Germany

Received 24 May 2010, in final form 31 August 2010
Published 27 September 2010
Online at stacks.iop.org/JPhysCM/22/415901

Abstract

We present the results of calculations of surface relaxations, rumplings, energetics, optical band gaps, and charge distribution for the $SrZrO_3$ and $PbZrO_3$ (001) and (011) surfaces using the *ab initio* code CRYSTAL and a hybrid description of exchange and correlation. We consider both SrO(PbO) and ZrO_2 terminations of the (001) surface and Sr(Pb), ZrO, and O terminations of the polar $SrZrO_3$ and $PbZrO_3$ (011) surfaces. On the (001) surfaces, we find that all upper and third layer atoms relax inward, while outward relaxations of all atoms in the second layer are found with the sole exception of the SrO-terminated $SrZrO_3$ (001) surface second layer O atom. Between all (001) and (011) surfaces the largest relaxations, more than 15% of the bulk lattice constant, are for the Sr- and Pb-terminated $SrZrO_3$ and $PbZrO_3$ (011) surface upper layer Sr and Pb atoms. Our calculated surface rumpling for the SrO- and PbO-terminated $SrZrO_3$ and $PbZrO_3$ (001) surfaces (6.77 and 3.32% of a_0) are by a factor of ten larger than the surface rumpling for the ZrO_2-terminated (001) surfaces (−0.72 and 0.38% of a_0, respectively). In contrast to the surface rumpling, the (001) surface energies are comparable and in the energy range from 0.93 eV/cell for the ZrO_2-terminated $PbZrO_3$ surface to 1.24 eV/cell for the ZrO_2-terminated $SrZrO_3$ surface. In contrast to the (001) surface, different terminations of the $SrZrO_3$ and $PbZrO_3$ (011) surfaces lead to very different surface energies ranging from 1.74 eV/cell for the Pb-terminated $PbZrO_3$ (011) surface to 3.61 eV/cell for the ZrO-terminated $SrZrO_3$ (011) surface. All our calculated (011) surface energies are considerably larger than the (001) surface energies. Our calculated optical band gap for the $SrZrO_3$ bulk, 5.31 eV, is in fair agreement with the experimental value of 5.6 eV. All our calculated optical band gaps for the $SrZrO_3$ and $PbZrO_3$ (001) and (011) surfaces are reduced with respect to the bulk. We predict a considerable increase in the Zr–O chemical bond covalency near the $SrZrO_3$ and $PbZrO_3$ (011) surfaces as compared both to the bulk and to the (001) surface.

(Some figures in this article are in colour only in the electronic version)

1. Introduction

Strontium zirconate $SrZrO_3$ is of technological interest because of applications in fuel cells, hydrogen gas sensors and steam electrolysis [1]. Lead zirconate $PbZrO_3$ has many technologically important applications including actuators, capacitors and charge storage devices [2–4]. For all these applications, the surface structure and the associated surface electronic and chemical properties are of primary importance. *Ab initio* calculations of $SrZrO_3$ and $PbZrO_3$ surface characteristics are useful to understand processes in which surfaces play a crucial role, such as the chemistry of surface reactions, interface phenomena, and adsorption.

In view of this technological importance, it is surprising that there have been neither experimental nor theoretical investigations of $SrZrO_3$ and $PbZrO_3$ (011) surface structure. Although experimental studies dealing with the $SrZrO_3$ (001) surface are still missing, the temperature dependence of the ferroelectric hysteresis and capacitance in $PbZrO_3$ epitaxial films has been investigated in the 4.2–400 K

temperature range [5]. $SrZrO_3$ and $PbZrO_3$ (001) surfaces have recently been studied theoretically by means of *ab initio* methods [6–10].

In contrast to ABO_3 perovskite (001) surfaces, their (011) surfaces are considerably less studied, both experimentally and theoretically. Most of the experimental work dealing with ABO_3 perovskite (011) surfaces was focused on the $SrTiO_3$ (011) surface using STM, UPS, XPS techniques, Auger spectroscopies, and LEED experiments [11–17]. The $SrTiO_3$ (011) surface, triggered by especially high technological importance of this perovskite, was also the most popular (011) surface for theoreticians, since four *ab initio* studies were performed for it during the last seven years using different density functional theory based methods, the Hartree–Fock (HF) method, as well as a hybrid description of exchange and correlation [18–21].

Regarding other ABO_3 perovskite (011) surfaces, Heifets *et al* [22] and Eglitis [23] investigated the atomic structure and charge redistribution of different terminations of $BaZrO_3$ (011) surfaces. Eglitis and Vanderbilt recently performed *ab initio* calculations based on hybrid HF and density functional theory (DFT) exchange functionals by using Becke's three-parameter method combined with the nonlocal correlation functionals of Perdew and Wang (B3PW) for the technologically important $BaTiO_3$ and $PbTiO_3$ (011) surfaces [24]. Finally, only two *ab initio* studies exist for the $CaTiO_3$ (011) surfaces. The *ab initio* study of $CaTiO_3$ (011) polar surfaces was performed by Zhang *et al* [25] and recently also by Eglitis and Vanderbilt [26].

According to the experimental results [27] $SrZrO_3$ undergoes three phase transitions: it is orthorhombic with space group P_{nma} below 970 K, and belongs to another orthorhombic space group C_{mcm} between 970 and 1020 K. At 1020 K, it transforms into tetragonal with space group $I4/_{mcm}$. Above 1360 K, it becomes cubic with space group $P_{m\bar{3}m}$. $PbZrO_3$ exhibits three different phases: a low temperature orthorhombic antiferroelectric phase stable up to 503 K, a rhombohedral ferroelectric phase stable at 503–506 K, and a cubic paraelectric phase above 506 K. For our $SrZrO_3$ and $PbZrO_3$ (001) and (011) surface calculations we chose the cubic phase because it is most extensively studied for other ABO_3 perovskites, such as, for example, $SrTiO_3$, $BaTiO_3$, $PbTiO_3$, $CaTiO_3$, and $BaZrO_3$ [19, 21–26]. The surface studies for other $SrZrO_3$ and $PbZrO_3$ low symmetry phases remain a challenging future problem.

2. Computational method

To perform the first-principles DFT–B3LYP calculations, we used the CRYSTAL computer code [28]. This code employs Gaussian-type functions (GTF) localized at atoms as the basis for an expansion of the crystalline orbitals. Features of the CRYSTAL code, which are most important for study of perovskite surfaces, are its ability to calculate the electronic structure of materials within both HF and Kohn–Sham (KS) Hamiltonians and implementation of the isolated 2D slab model without its artificial repetition along the z-axis. However, in order to employ the linear combination of atomic orbitals (LCAO)-GTF method, it is desirable to have optimized basis sets (BS). The optimization of such BSs for $SrTiO_3$, $BaTiO_3$ and $PbTiO_3$ perovskites was developed and discussed in [29]. In this paper, for O atoms, we used this new BS which differs from previous calculations [30, 31] by inclusion of polarizable d-orbitals on O ions.

Our calculations were performed using the hybrid exchange–correlation B3LYP functional involving a hybrid of nonlocal Fock exact exchange, LDA exchange and Becke's gradient corrected exchange functional [32], combined with the nonlocal gradient corrected correlation potential by Lee–Yang–Parr [33]. The Hay–Wadt small-core effective core pseudopotentials (ECP) were adopted for Sr and Zr atoms [34]. The small-core ECPs replace only inner core orbitals, but orbitals for sub-valence electrons as well as for valence electrons are calculated self-consistently. Light oxygen atoms were treated with the all-electron BS [29].

The reciprocal space integration was performed by sampling the Brillouin zone of the five-atom cubic unit cell with the $5 \times 5 \times 1$ Pack–Monkhorst net [35], that provides the balanced summation in direct and reciprocal spaces. To achieve high accuracy, large enough tolerances of 7, 8, 7, 7, 14 were chosen for the Coulomb overlap, Coulomb penetration, exchange overlap, the first exchange pseudo-overlap, and for the second exchange pseudo-overlap, respectively [28].

The $SrZrO_3$ and $PbZrO_3$ (001) surfaces were modeled with two-dimensional (2D) slabs, consisting of several planes perpendicular to the [001] crystal direction. (Henceforth, we shall use $SrZrO_3$ for presentation purposes, but everything that is said will apply equally to the $PbZrO_3$ case.) The CRYSTAL code allowed us to avoid artificial periodicity along the Oz direction and to perform simulations for stand-alone 2D slabs. To simulate $SrZrO_3$ (001) surfaces, we used symmetrical (with respect to the mirror plane) slabs consisting of nine alternating SrO and ZrO_2 layers (see figure 1). One of these slabs was terminated by SrO planes and consisted of a supercell containing 22 atoms. The second slab was terminated by ZrO_2 planes and consisted of a supercell containing 23 atoms. These slabs are non-stoichiometric, with unit cell formulas $Sr_5Zr_4O_{13}$ and $Sr_4Zr_5O_{14}$, respectively. These two (SrO and ZrO_2) terminations are the only two possible flat and dense (001) surfaces in $SrZrO_3$ perovskite lattice structure. The sequence of layers with [001] orientation in $SrZrO_3$ is illustrated in figure 1.

Unlike the $SrZrO_3$ (001) neutral surface, the problem in modeling the $SrZrO_3$ (011) polar surface (see figure 2) is that it consists of charged planes, O–O or SrZrO. If one assumes fixed ionic charges O^{2-}, Zr^{4+}, and Sr^{2+}, then modeling of the $SrZrO_3$ (011) surface exactly as would be obtained from a perfect crystal cleavage leads either to an infinite macroscopic dipole moment perpendicular to the surface, when the slab is terminated by planes of different kinds (O_2 and SrZrO) (stoichiometric slab) (see figure 3(a)), or to infinite charge, when it is terminated by the same type of crystalline planes (O_2–O_2 (see figure 3(b)) or SrZrO–SrZrO (see figure 3(c))) (non-stoichiometric slab). It is known that such crystal terminations make the surface unstable [36, 37].

This was the reason why in our $SrZrO_3$ (011) surface calculations, in order to get the neutral slab, we removed

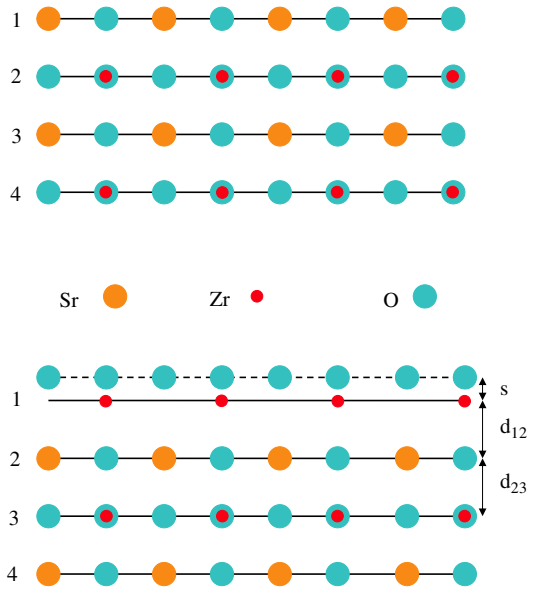

Figure 1. Side view of $SrZrO_3$ (001) surfaces. (a) SrO-terminated surface. (b) ZrO_2-terminated surface with definitions of surface rumpling s and the near-surface interplanar separations Δd_{12} and Δd_{23}.

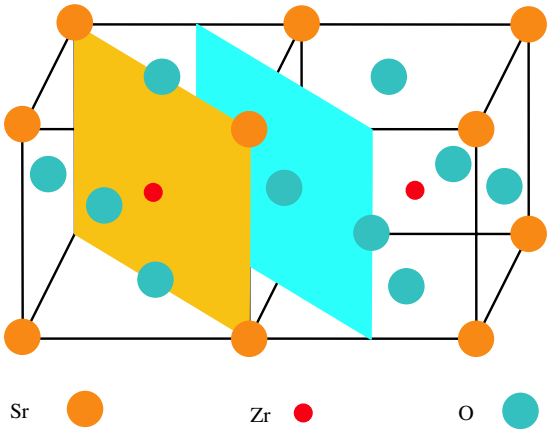

Figure 2. Sketch of the cubic $SrZrO_3$ perovskite structure showing two (011) cleavage planes that give rise to charged SrZrO and O_2 (011) surfaces.

the O atom from the upper and lower layers of the nine-layer symmetric O–O terminated non-stoichiometric slab (see figure 3(d)), and Sr (see figure 3(e)) or both Zr and O atoms (see figure 3(f)) from the upper and lower layers of the SrZrO-terminated non-stoichiometric slab. Thereby, in our calculations, the ZrO-terminated symmetric nine-layer non-stoichiometric slab consisted of a supercell containing 21 atoms, and finally, the Sr- and O-terminated symmetric non-stoichiometric nine-layer slabs consisted of supercells containing 19 and 20 atoms, respectively.

In the present work, we define the unrelaxed surface energy of a given surface termination Ω to be one half of the energy needed to cleave the crystal rigidly into an unrelaxed surface Ω and an unrelaxed surface with the complementary

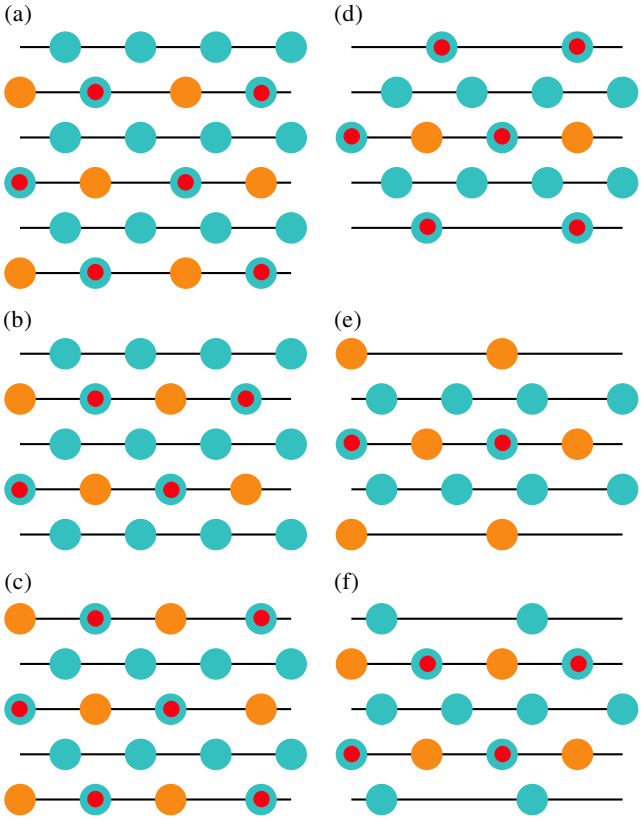

Figure 3. Possible (011) surface slab models considered in the text. Slabs obtained by simple cleavage yielding: (a) mixed, (b) O-terminated and (c) SrZrO-terminated polar surfaces. Slabs with nonpolar termination: (d) O-terminated, (e) ZrO-terminated and (f) Sr-terminated.

termination Ω′. For $SrZrO_3$, the unrelaxed surface energies of the complementary SrO- and ZrO_2-terminated (001) surfaces are thus equal by definition, as are those of the ZrO- and Sr-terminated (011) surfaces. The relaxed surface energy is defined to be the energy of the unrelaxed surface plus the (negative) surface relaxation energy.

In order to calculate the $SrZrO_3$ (001) surface energy, we started with the cleavage energy for unrelaxed SrO- and ZrO_2-terminated (001) surfaces. Surfaces with both terminations simultaneously arise under (001) cleavage of the crystal, and we adopt the convention that the cleavage energy is equally distributed between the created surfaces. In our calculations, the nine-layer SrO-terminated (001) slab with 22 atoms and the ZrO_2-terminated one with 23 atoms represent, together, nine bulk unit cells (45 atoms) so that

$$E_{\text{surf}}^{(\text{unr})}(\Omega) = \tfrac{1}{4}[E_{\text{slab}}^{(\text{unr})}(\text{SrO}) + E_{\text{slab}}^{(\text{unr})}(\text{ZrO}_2) - 9E_{\text{bulk}}], \quad (1)$$

where Ω denotes SrO or ZrO_2, $E_{\text{slab}}^{(\text{unr})}(\Omega)$ are the unrelaxed energies of the SrO- or ZrO_2-terminated (001) slabs, E_{bulk} is the energy per bulk unit cell, and the factor of $\frac{1}{4}$ comes from the fact that we create four surfaces upon the cleavage procedure. Next, we can calculate the relaxation energies for each of SrO and ZrO_2 terminations, when both sides of the slabs relax,

according to

$$E_{\rm rel}(\Omega) = \tfrac{1}{2}[E^{\rm (rel)}_{\rm slab}(\Omega) - E^{\rm (unr)}_{\rm slab}(\Omega)], \quad (2)$$

where $E^{\rm (rel)}_{\rm slab}(\Omega)$ is the slab energy after relaxation (and again Ω = SrO or ZrO_2). The surface energy is then defined as a sum of the cleavage and relaxation energies,

$$E_{\rm surf}(\Omega) = E^{\rm (unr)}_{\rm surf}(\Omega) + E_{\rm rel}(\Omega). \quad (3)$$

In order to calculate the $SrZrO_3$ (011) surface energies for the ZrO- and Sr-terminated surfaces, we consider the cleavage of eight bulk unit cells (40 atoms) to result in the ZrO- and Sr-terminated slabs, containing 21 and 19 atoms, respectively. We again divide the cleavage energy equally between these two surfaces and obtain

$$E^{\rm (unr)}_{\rm surf}(\Omega) = \tfrac{1}{4}[E^{\rm (unr)}_{\rm slab}({\rm Sr}) + E^{\rm (unr)}_{\rm slab}({\rm ZrO}) - 8E_{\rm bulk}], \quad (4)$$

where Ω denotes Sr or ZrO, $E^{\rm (unr)}_{\rm slab}(\Omega)$ is the energy of the unrelaxed Sr- or ZrO-terminated (011) slab, and $E_{\rm bulk}$ is the $SrZrO_3$ energy per bulk unit cell.

Finally, when we cleave the $SrZrO_3$ crystal in another way, we obtain two identical O-terminated (011) surface slabs containing 20 atoms each. This allows us to simplify the calculations since the unit cell of the nine-plane O-terminated (011) slab contains four bulk unit cells. Therefore, the relevant surface energy is

$$E_{\rm surf}({\rm O}) = \tfrac{1}{2}[E^{\rm (rel)}_{\rm slab}({\rm O}) - 4E_{\rm bulk}], \quad (5)$$

where $E_{\rm surf}$(O) and $E^{\rm (rel)}_{\rm slab}$(O) are the surface energy and the relaxed slab total energy for the O-terminated (011) surface.

3. Results of calculations

3.1. $SrZrO_3$ and $PbZrO_3$ bulk atomic and electronic structure

As a starting point of our calculations, we calculated the $SrZrO_3$ (4.195 Å), and $PbZrO_3$ (4.220 Å) bulk lattice constants. Our calculated lattice constant for $SrZrO_3$ (4.195 Å) is slightly larger than the experimental value of 4.109 Å [38]. Also our calculated lattice constant for $PbZrO_3$ (4.220 Å) is overestimated only by 1.4% in comparison to the experimental result (4.161 Å [39]). Thus, the computational approach used in the present study can be established as appropriate. We used the theoretical $SrZrO_3$ and $PbZrO_3$ bulk lattice constants in the following (001) and (011) surface structure calculations. To characterize the chemical bonding and covalency effects, we used a standard Mulliken population analysis for the effective atomic charges Q and other local properties of electronic structure as described, for example, in [40, 41]. Our calculated effective charges for the $SrZrO_3$ bulk are (+1.880e) for the Sr atom, (+2.174e) for the Zr atom, and (−1.351e) for the O atom (see table 1). Our calculated effective charges for the $PbZrO_3$ perovskite bulk are (+1.368e) for the Pb atom, (+2.111e) for the Zr atom, and (−1.160e) for the O atom. The bond population of the chemical bonding between Zr and O atoms is (+0.092e) in $SrZrO_3$, and slightly larger (+0.106e) in $PbZrO_3$. The bond populations between Sr and O atoms in $SrZrO_3$ (0.002e) and between Pb and O atoms in $PbZrO_3$ (0.030e) are much smaller. Finally, the bond populations between O and O atoms in $SrZrO_3$ (−0.008e) and in $PbZrO_3$ (−0.020e) are negative, which indicates repulsion between O–O atoms (see table 1).

Table 1. Effective charges Q and bond populations P of atoms in $SrZrO_3$ and $PbZrO_3$ bulk calculated by means of the hybrid B3LYP method.

$SrZrO_3$ bulk			$PbZrO_3$ bulk		
Ion	Property	B3LYP	Ion	Property	B3LYP
Sr	Q	+1.880	Pb	Q	+1.368
	P	+0.002		P	+0.030
O	Q	−1.351	O	Q	−1.160
	P	+0.092		P	+0.106
Zr	Q	+2.174	Zr	Q	+2.111

Table 2. The calculated optical band gaps (in electron volts) for the $SrZrO_3$ and $PbZrO_3$ bulk using different exchange–correlation functionals.

Method	$SrZrO_3$	$PbZrO_3$
B3LYP	5.31	5.63
HF	13.54	13.89
PWGGA	3.53	3.86
PBE	3.52	3.86

The calculated forbidden optical band gap for $SrZrO_3$ and $PbZrO_3$ crystals depends considerably on the choice of the exchange–correlation functional (see table 2). As usual [42–44], the Hartree–Fock band gap is considerably overestimated, whereas PWGGA and PBE are underestimated. The best results are obtained for the hybrid B3LYP method used later in this paper. Our calculated optical band gap by means of the B3LYP method for the $SrZrO_3$ bulk, 5.31 eV, is in an excellent agreement with the experimentally measured $SrZrO_3$ optical band gap of 5.6 eV [45].

3.2. $SrZrO_3$ and $PbZrO_3$ (001) surface structure

Our calculated atomic displacements for the $SrZrO_3$ and $PbZrO_3$ (001) surface upper three layers are presented in table 3. According to the results of our calculations all atoms of the first and third $SrZrO_3$ and $PbZrO_3$ surface layer relax inwards, i.e. towards the bulk, while outward relaxations of all atoms in the second layer are found for both $SrZrO_3$ and $PbZrO_3$ (001) terminations. The only exception is inward relaxation of the SrO-terminated $SrZrO_3$ (001) surface second layer oxygen atom by a very small magnitude of 0.05% of a_0. The relaxations of the surface upper layer metal atoms for SrO- and PbO-terminated $SrZrO_3$ and $PbZrO_3$ (001) surfaces are much larger than that of oxygen atoms which leads to a considerable rumpling (see table 4) of the outermost plane (6.77% and 3.32% of a_0, respectively). Our calculated surface rumplings for SrO- and PbO-terminated $SrZrO_3$ and $PbZrO_3$ (001) surfaces (6.77% and 3.32% of a_0) are approximately ten times larger than the surface rumplings for ZrO_2-terminated $SrZrO_3$ and $PbZrO_3$ (001) surfaces (−0.72% and 0.38% of a_0, respectively). The inward relaxation of the (001) surface upper and third layer atoms and upward relaxation of the second

Table 3. Atomic relaxation (in per cent of the bulk lattice constant) for the ZrO_2-terminated $SrZrO_3$ and $PbZrO_3$ (001) surfaces, as well as for SrO- or PbO-terminated $SrZrO_3$ or $PbZrO_3$ (001) surfaces calculated by the hybrid B3LYP method. Positive (negative) values refer to displacements in the direction outwards from (inwards to) the surface.

	$SrZrO_3$				$PbZrO_3$			
	SrO-terminated		ZrO_2-terminated		PbO-terminated		ZrO_2-terminated	
N	Ion	This study	Ion	This study	Ion	This study	Ion	This study
1	Sr	−7.63	Zr	−1.38	Pb	−5.69	Zr	−2.37
	O	−0.86	O	−2.10	O	−2.37	O	−1.99
2	Zr	+0.86	Sr	+2.81	Zr	+0.57	Pb	+4.36
	O	−0.05	O	+0.91	O	+0.09	O	+1.04
3	Sr	−1.53	Zr	−0.04	Pb	−0.47	Zr	−0.47
	O	−0.45	O	−0.05	O	−0.47	O	−0.28

Table 4. Calculated surface rumpling s, and relative displacements Δd_{ij} between the three near-surface planes, for the SrO-, PbO- and ZrO_2-terminated $SrZrO_3$ and $PbZrO_3$ (001) surfaces. Units are per cent of the bulk lattice constant. *Ab initio* calculation results and experimental data for other ABO_3 perovskites are listed for comparison.

Crystal	Termination	s	Δd_{12}	Δd_{23}	Termination	s	Δd_{12}	Δd_{23}
$SrZrO_3$	SrO-term	+6.77	−8.49	+2.39	ZrO_2-term	−0.72	−4.19	+2.85
$SrZrO_3$ [6] [LDA]	SrO-term	+7.9	−9.1	+3.2	ZrO_2-term	−0.7	−6.1	+4.2
$SrZrO_3$ [6] [GGA]	SrO-term	+7.8	−9.3	+3.3	ZrO_2-term	+0.3	−7.4	+4.9
$PbZrO_3$ [10]	PbO-term	+6.88	−8.6	+3.4	ZrO_2-term	+1.1	−7.1	+4.9
$BaZrO_3$ [23]	BaO-term	+3.07	−4.77	+0.48	ZrO_2-term	+0.09	−3.73	+1.97
$SrTiO_3$ [21]	SrO-term	+5.66	−6.58	+1.75	TiO_2-term	+2.12	−5.79	+3.55
$SrTiO_3$ [46]	SrO-term	$+4.1 \pm 2$	-5 ± 1	$+2 \pm 1$	TiO_2-term	$+2.1 \pm 2$	$+1 \pm 1$	-1 ± 1
$SrTiO_3$ [47]	SrO-term	+4.1	+2.6	+1.3	TiO_2-term	+2.6	+1.8	+1.3
$BaTiO_3$ [24]	BaO-term	+1.37	−3.74	+1.74	TiO_2-term	+2.73	−5.59	+2.51
$PbTiO_3$ [24]	PbO-term	+3.51	−6.89	+3.07	TiO_2-term	+3.12	−8.13	+5.32
$CaTiO_3$ [26]	CaO-term	+7.89	−9.43	+1.12	TiO_2-term	+1.61	−4.46	+2.75

layer atoms, are in line with the results of our previous *ab initio* calculations for other ABO_3 perovskites, such as $SrTiO_3$, $BaTiO_3$, $PbTiO_3$, $CaTiO_3$, and $BaZrO_3$ [21, 23, 24, 26]. The only two exceptions there were outward relaxation of the TiO_2-terminated $PbTiO_3$ (001) surface first layer O atom by 0.31% of a_0, and outward relaxation of the SrO-terminated $SrTiO_3$ (001) surface upper layer O atom by 0.84% of a_0. According to the results of current calculations for $SrZrO_3$ and $PbZrO_3$, as well as the results of our previous *ab initio* calculations for $SrTiO_3$, $BaTiO_3$, $PbTiO_3$, $CaTiO_3$ and $BaZrO_3$ (001) surfaces [21, 23, 24, 26], the upper layer metal atom displacement for an AO-terminated ABO_3 (001) surface is always larger than for the BO_2-terminated (001) surface. Only for the $BaTiO_3$ crystal, was the Ti atom inward displacement for the TiO_2-terminated $BaTiO_3$(001) surface, 3.08% of a_0, larger than the inward displacement for the Ba atom on the BaO-terminated $BaTiO_3$ (001) surface, 1.99% of a_0. The two largest metal atom displacements between all our calculated AO-terminated ABO_3 (001) surfaces was for the CaO-terminated $CaTiO_3$ (001) surface, where the Ca atom inward displacement was 8.31% of a_0 and for $SrZrO_3$, where the Sr displacement for the SrO-terminated (001) surface was 7.63% of a_0.

In order to compare the calculated surface structures with experimental results, the surface rumpling s (the relative displacement of oxygen with respect to the metal in the surface layer) and the changes in interlayer distances Δd_{12} and Δd_{23} (1, 2, and 3 are the numbers of near-surface layers) are presented in table 4. Our calculations of the interlayer distances are based on the positions of relaxed metal ions (figure 1), which are known to be much stronger electron scatters than oxygen ions [46]. From table 4 one can see that all $SrZrO_3$ and $PbZrO_3$ (001) surfaces show the reduction of interlayer distance Δd_{12} and expansion of Δd_{23}. For all $SrZrO_3$ and $PbZrO_3$ surface (001) terminations the reduction of interlayer distance d_{12} is considerably larger than the expansion of the interlayer distance d_{23}.

Our calculated surface rumpling s for $SrTiO_3$, $BaTiO_3$, $PbTiO_3$, $CaTiO_3$, and $BaZrO_3$ perovskite (001) surfaces was always positive [21, 23, 24, 26] (see table 4). In contrast to our previous results, the current *ab initio* calculated surface rumpling for the ZrO_2-terminated $SrZrO_3$ (001) surface is negative. Moreover, our calculated negative surface rumpling for the ZrO_2-terminated $SrZrO_3$ (001) surface (−0.72% of a_0) is in a surprisingly good agreement with the earlier LDA calculation result by Wang and Arai [6] (−0.7% of a_0), however it is in contrast to the GGA result for the ZrO_2-terminated $SrZrO_3$(001) surface rumpling by the same authors (+0.3% of a_0).

To the best of our knowledge there are no experimental measurements for $SrZrO_3$ and $PbZrO_3$ (001) surfaces with which we can compare our calculated values of s, Δd_{12}, and Δd_{23}. Even when such data do exist, they are sometimes contradictory, as is the case for the SrO-terminated $SrTiO_3$ (001) surface, where existing LEED [46] and RHEED [47] experiments contradict each other regarding the sign of Δd_{12}.

Table 5. Calculated absolute magnitudes of atomic displacements D (in Å), the effective atomic charges Q (in e) and the bond populations P between nearest Me–O atoms (in e) for the ZrO_2- and SrO-terminated $SrTiO_3$ and ZrO_2- and PbO-terminated $PbZrO_3$ (001) surfaces.

		$SrZrO_3$				$PbZrO_3$			
Layer	Property	Ion	ZrO_2-terminated	Ion	SrO-terminated	Ion	ZrO_2-terminated	Ion	PbO-terminated
1	D	Zr	−0.058	Sr	−0.320	Zr	−0.100	Pb	−0.240
	Q		+2.196		+1.858		+2.165		+1.299
	P		0.114		+0.008		+0.116		+0.064
	D	O	−0.088	O	−0.036	O	−0.084	O	−0.100
	Q		−1.277		−1.524		−1.171		−1.199
	P		−0.002		+0.042		+0.046		+0.048
2	D	Sr	+0.118	Zr	+0.036	Pb	+0.184	Zr	+0.024
	Q		+1.869		+2.227		+1.357		+2.159
	P		0.002		+0.076		+0.022		+0.092
	D	O	+0.038	O	−0.002	O	+0.044	O	+0.004
	Q		−1.287		−1.398		−1.103		−1.172
	P		0.094		+0.002		+0.098		+0.026
3	D	Zr	−0.001 66	Sr	−0.064	Zr	−0.020	Pb	−0.020
	Q		+2.172		+1.877		+2.116		+1.349
	P		0.102		+0.002		+0.124		+0.036
	D	O	−0.002	O	−0.0188	O	−0.012	O	−0.020
	Q		−1.331		−1.361		−1.148		−1.165
	P		0.002		+0.094		+0.036		+0.110

Table 6. Calculated optical band gap for $SrZrO_3$ and $PbZrO_3$ (001) and (011) surfaces (in eV).

Termination	$SrZrO_3$ gap	Termination	$PbZrO_3$ gap
Bulk	5.31	Bulk	5.63
SrO(001)	5.04	PbO(001)	3.86
ZrO_2 (001)	4.91	ZrO_2 (001)	4.60
O(011)	5.27	O(011)	4.99
Sr(011)	4.40	Pb(011)	4.39
ZrO(011)	5.07	ZrO(011)	5.16

We begin discussion of the electronic structure of SrO-, PbO- and ZrO_2-terminated $SrZrO_3$ and $PbZrO_3$(001) surfaces with the analysis of charge redistribution in near-surface planes. The calculated atomic displacements, effective static atomic charges (calculated using Mulliken population analysis) and bond populations between nearest metal and oxygen atoms are presented in table 5. First of all, note that the effective static charges of Sr (+1.858e) on the SrO-terminated $SrTiO_3$ (001) surface are close to the +2e formal ionic charges, whereas that of Pb (+1.299e) on the PbO-terminated $PbTiO_3$ (001) surface is considerably smaller. Ti and O effective static charges are also much smaller than the formal ionic charges, similarly to the bulk, which results from the Ti–O covalent bonding. Comparing with the very small bulk Sr–O (+0.002e) and Pb–O (+0.030e) bond populations from table 1, we see that the Sr–O and Pb–O bond populations near the SrO- and PbO-terminated $SrZrO_3$ and $PbZrO_3$ (001) surfaces are four and more than two times larger than in the bulk (see table 5). The major effect observed near the ZrO_2-terminated $SrZrO_3$ and $PbZrO_3$ (001) surfaces is a strengthening of the Zr–O chemical bond. Recall from table 1 that the Zr and O effective charges (+2.174e and −1.351e) in $SrZrO_3$ and (+2.111e and −1.160e) in $PbZrO_3$ bulk are much smaller than expected in an ideal ionic model and that the Zr–O bond population is (+0.092e) and (+0.106e) in $SrZrO_3$ and $PbZrO_3$, respectively.

Table 7. Calculated cleavage, relaxation, and surface energies for $SrZrO_3$ and $PbZrO_3$ (001) and (011) surfaces (in eV/surface cell). In both cases and for both materials three near-surface planes were relaxed.

Surface	Termination	E_{cleav}	E_{rel}	E_{surf}
$SrZrO_3$ (001)	ZrO_2	1.56	−0.32	1.24
	SrO	1.56	−0.43	1.13
$SrZrO_3$ (011)	ZrO	4.94	−1.33	3.61
	Sr	4.94	−2.73	2.21
	O	3.77	−1.54	2.23
$PbZrO_3$ (001)	ZrO_2	1.20	−0.27	0.93
	PbO	1.20	−0.20	1.00
$PbZrO_3$ (011)	ZrO	3.38	−1.49	1.89
	Pb	3.38	−1.64	1.74
	O	3.14	−1.29	1.85

Table 5 shows that the Zr–O bond population for the ZrO_2-terminated $SrZrO_3$ and $PbZrO_3$ (001) surfaces is considerably larger than the associated bulk value.

We should stress here remarkable agreement of our B3LYP calculated $SrZrO_3$ optical bulk band gap, 5.31 eV, with the experimental value, 5.6 eV [45]. This is in a sharp contrast with the typical HF overestimate of the optical bulk band gap, 13.54 eV, and DFT underestimate (see table 2). The calculated optical band gap for the SrO- , PbO- , and ZrO_2-terminated $SrZrO_3$ and $PbZrO_3$ (001) surfaces becomes smaller with respect to the bulk optical band gap (see table 6). The narrowest optical band gap between all $SrZrO_3$ and $PbZrO_3$ (001) surfaces, according to our B3LYP calculations, is for the PbO-terminated $PbZrO_3$(001) surface (3.86 eV). In contrast, the optical band gap for the SrO-terminated $SrZrO_3$ (001) surface is considerably less, only by 0.27 eV, reduced in comparison to the calculated bulk value of 5.31 eV.

The surface energies of the relaxed $SrZrO_3$ and $PbZrO_3$ (001) surfaces, presented in table 7, were computed using

Table 8. Atomic relaxation of the $SrZrO_3$ and $PbZrO_3$ (011) surfaces (in per cent of the bulk lattice constant) for the three terminations calculated by means of the *ab initio* B3LYP method. A positive sign corresponds to outward atomic displacements (towards the vacuum).

$SrZrO_3$ (011) surface				$PbZrO_3$ (011) surface			
Layer	Ion	Δz	Δy	Layer	Ion	Δz	Δy
ZrO-terminated $SrZrO_3$ (011) surface				ZrO-terminated $PbZrO_3$ (011) surface			
1	Zr	−6.16		1	Zr	−6.87	
1	O	+4.36		1	O	+4.27	
2	O	−0.38		2	O	−0.24	
3	Sr	−1.94		3	Pb	−2.37	
3	O	−5.69		3	O	−5.69	
3	Zr	−0.40		3	Zr	−0.02	
Sr-terminated $SrZrO_3$ (011) surface				Pb-terminated $PbZrO_3$ (011) surface			
1	Sr	−15.73		1	Pb	−15.17	
2	O	+1.24		2	O	−0.57	
3	Zr	+0.10		3	Zr	−0.66	
3	O	−0.95		3	O	+2.37	
3	Sr	−0.48		3	Pb	+3.41	
O-terminated $SrZrO_3$ (011) surface				O-terminated $PbZrO_3$ (011) surface			
1	O	−6.56	−3.58	1	O	−6.61	−3.55
2	Zr	+1.45	−4.29	2	Zr	+0.73	−4.53
2	Sr	−1.43	−0.24	2	Pb	+0.73	−3.79
2	O	+4.29	+7.87	2	O	+4.29	+7.94
3	O	−0.10	+1.74	3	O	−0.19	+1.66

equations (1)–(3). The surface energies calculated for AO- and ZrO_2-terminated (001) surfaces demonstrate only a small difference, which means that both terminations could co-exist. Nevertheless, the energy computed for the ZrO_2-terminated $SrZrO_3$ (001) surface (1.24 eV/cell) is a little bit larger than that for the SrO-termination (1.13 eV/cell), in contrast to the $PbZrO_3$ crystal where the ZrO_2-terminated (001) surface is energetically slightly more favorable.

In comparison, according to our earlier *ab initio* calculation results, the (001) surface energies for $SrTiO_3$, $BaTiO_3$, $PbTiO_3$, $CaTiO_3$ and $BaZrO_3$ [21, 23, 24, 26] were in the energy range between 0.74 eV/cell for the TiO_2-terminated $PbTiO_3$ (001) surface and 1.31 eV/cell for the ZrO_2-terminated $BaZrO_3$ (001) surface. The BaO (1.30 eV/cell) and ZrO_2-terminated (1.31 eV/cell) $BaZrO_3$ (001) surface energies almost coincide, but the largest calculated energy differences were for the CaO (0.94 eV/cell) and TiO_2-terminated (1.13 eV/cell) $CaTiO_3$ (001) surfaces. Nevertheless, all our previously calculated $SrTiO_3$, $BaTiO_3$, $PbTiO_3$, $CaTiO_3$ and $BaZrO_3$ (001) surface energies were rather close, which means that both AO and BO_2 terminations could exist simultaneously.

3.3. $SrZrO_3$ and $PbZrO_3$ (011) surface energies and atomic structures

Unlike the $SrZrO_3$ and $PbZrO_3$ (001) surfaces, we see that different terminations of the $SrZrO_3$ (011) surface lead to great differences in the surface energies (see table 7). The surface energy difference between ZrO- and Sr-terminated $SrZrO_3$ (011) surfaces is equal to 1.40 eV/cell, which is larger than any of the $SrZrO_3$ or $PbZrO_3$ (001) surface energies. Among all the $SrZrO_3$ and $PbZrO_3$ (011) surfaces the Pb-terminated $PbZrO_3$ (011) surface has the lowest surface energy. The surface energy per unit cell for the Pb-terminated $PbZrO_3$ (011) surface 1.74 eV/cell is by a factor of two smaller than the ZrO-terminated $SrZrO_3$ surface energy 3.61 eV/cell. In contrast to the $SrZrO_3$(011) surfaces, the (011) surface energies are very close for the $PbZrO_3$ crystal. Namely, the Pb-terminated $PbZrO_3$ surface has the lowest energy 1.74 eV/cell between all $PbZrO_3$ (011) surfaces, while the ZrO-terminated $PbZrO_3$ (011) surface has the highest surface energy 1.89 eV/cell.

According to the results of our previous *ab initio* calculations for $SrTiO_3$, $BaTiO_3$, $PbTiO_3$, $CaTiO_3$, and $BaZrO_3$(011) surfaces [21, 23, 24, 26], the largest surface energy difference between two different (011) surface terminations was for the $BaTiO_3$ (1.52 eV/cell). The largest (011) surface energy was for the Ba-terminated $BaTiO_3$ (011) surface (3.24 eV/cell), while the smallest (011) surface energy was for the TiO-terminated $PbTiO_3$ (011) surface (1.36 eV/cell). According to the results of our previous *ab initio* calculations, among all the $SrTiO_3$, $BaTiO_3$, $CaTiO_3$, and $BaZrO_3$ (011) surfaces, the lowest surface energy was always for the O-terminated (011) surface, while the TiO-terminated surface was the lowest energy (011) surface for the $PbTiO_3$ crystal.

An idea about the nature of the relaxed $SrZrO_3$ and $PbZrO_3$ (011) surfaces can be obtained from figure 3. On the ZrO-terminated $SrZrO_3$ and $PbZrO_3$ (011) surface Zr atoms move inward by 6.16 and 6.87% of a_0, respectively, whereas O atoms move outward by 4.36 and 4.27% of a_0 (see table 8), which leads to a large ZrO-terminated surface rumpling (see table 9). Also the other ZrO-terminated $SrZrO_3$ and $PbZrO_3$ (011) surface second and third layer atom displacement directions, and for the third layer O atoms even the displacement magnitude 5.69% of a_0 coincide. On the Sr-terminated $SrZrO_3$ and Pb-terminated $PbZrO_3$ (011) surfaces the upper layer Sr and Pb atoms move very strongly inwards by 15.73 and 15.17% of a_0. These Sr and Pb atomic displacement magnitudes are the largest atomic displacement magnitudes

Table 9. Surface rumpling s and relative displacements Δd_{ij} (in per cent of the bulk lattice constant a_0) for the three near-surface planes on the ZrO- and O-terminated $SrZrO_3$ and $PbZrO_3$ (011) surfaces. Our *ab initio* calculation results for other ABO_3 perovskites are listed for comparison.

Crystal	Termination	s	Δd_{12}	Δd_{23}	Termination	Δd_{12}	Δd_{23}
$SrZrO_3$	ZrO-term	+10.52	−5.78	+0.02	O-term	−8.01	+1.55
$PbZrO_3$	ZrO-term	+11.14	−6.63	−0.22	O-term	−7.34	+0.92
$BaZrO_3$	ZrO-term	+9.96	−6.32	−1.19	O-term	−7.44	+0.19
$SrTiO_3$ [21]	TiO-term	+11.28	−7.18	−0.67	O-term	−5.59	−0.23
$BaTiO_3$	TiO-term	+10.47	−6.84	−1.02	O-term	−5.25	−1.05
$PbTiO_3$	TiO-term	+11.43	−7.72	−0.71	O-term	−7.57	+0.61
$CaTiO_3$ [26]	TiO-term	+11.81	−6.70	+0.34	O-term	−5.84	+0.29

among all our calculated $SrZrO_3$ and $PbZrO_3$ (011) surface atoms. The displacement directions of all second and third layer atoms for the Sr-terminated $SrZrO_3$ (011) surface are opposite to the displacement directions of all corresponding atoms in the Pb-terminated $PbZrO_3$ (011) surface second and third layers. The O atoms in the top layer of the O-terminated $SrZrO_3$ and $PbZrO_3$ (011) surface move inward by almost the same magnitudes 6.56 and 6.61% of a_0, and also along the surface, again, by almost equal, but approximately two times smaller displacement magnitudes of 3.58 and 3.55% of a_0. The displacement directions of all second and third layer atoms on the O-terminated $SrZrO_3$ and $PbZrO_3$ (011) surface coincide, with the sole exception of the second layer Sr atom on the O-terminated $SrZrO_3$ (011) surface, which moves inwards by 1.43% of a_0, while the corresponding Pb atom on the O-terminated $PbZrO_3$ (011) surface moves outwards by 0.73% of a_0.

Our calculated surface rumplings for ZrO-terminated $SrZrO_3$, $PbZrO_3$, and $BaZrO_3$ (011), as well as for the TiO-terminated $SrTiO_3$, $BaTiO_3$, $PbTiO_3$, and $CaTiO_3$ (011) surfaces [21, 23, 24, 26] are very large, and in the range from 9.96% of a_0 for the ZrO-terminated $BaZrO_3$(011) surface to 11.81% of a_0 for the TiO-terminated $CaTiO_3$ (011) surface (see table 9). According to the results of our *ab initio* calculations for ZrO-terminated $SrZrO_3$, $PbZrO_3$, and $BaZrO_3$, as well as for TiO-terminated $SrTiO_3$, $BaTiO_3$, $PbTiO_3$ and $CaTiO_3$ (011) surfaces, the compression between first and second layers is between 5.78 and 7.72% of a_0. In contrast to a large compression of the first and second planes, the compression between second and third planes is much smaller, and in the range from 1.19% of a_0 for the ZrO-terminated $BaZrO_3$ (011) surface to 0.22% of a_0 for the ZrO-terminated $PbZrO_3$ (011) surface. In contrast, ZrO-terminated $SrZrO_3$ and TiO-terminated $CaTiO_3$ (011) surfaces are expanded by 0.02% of a_0 and 0.34% of a_0, respectively.

3.4. $SrZrO_3$ and $PbZrO_3$ (011) surface charge distributions, chemical bondings, and band structure

The interatomic bond populations for three possible $SrZrO_3$ and $PbZrO_3$ (011) surface terminations are given in table 10. The major effect observed here is a strong increase of the Zr–O chemical bonding near the O-terminated (011) surface as compared to already large bonding in the bulk (0.092e and 0.106e) for $SrZrO_3$ and $PbZrO_3$. For the O-terminated $SrZrO_3$ and $PbZrO_3$ (011) surfaces the O(I)–Zr(II) bond population is as large as 0.154e and 0.198e, i.e., by a factor of one and half and two larger than that in the $SrZrO_3$ and $PbZrO_3$ bulk. Our calculations demonstrate that for the ZrO-terminated $SrZrO_3$ and $PbZrO_3$ (011) surfaces, the Zr–O bond populations are larger in the direction perpendicular to the surface (0.246e and 0.252e) than in-plane (0.142e and 0.148e) (see table 10). There are no O atoms on the Sr- and Pb-terminated $SrZrO_3$ and $PbZrO_3$ (011) surfaces. However, the bond population between Pb(I) and O(II) atoms 0.120e is much larger than in the $PbZrO_3$ bulk and also considerably larger than near the PbO-terminated (001) surface.

We calculated the Mulliken effective charges Q, and their changes ΔQ, with respect to the bulk values for atoms near the surface (see table 11) for the various $SrZrO_3$ and $PbZrO_3$ (011) surface terminations. On the ZrO-terminated $SrZrO_3$ and $PbZrO_3$ (011) surfaces, the charge on the surface Zr atom is seen to be slightly increased relative to the bulk (+0.003e and +0.074e), while the Sr and Pb atoms in the third layer lose (−0.017e and −0.068e), respectively. Zr atom charges in the third layer increased relative to the bulk (+0.019e and +0.051e). The largest charge change (+0.198e and +0.106e) is observed for subsurface O atoms giving a large positive change of +0.396e and +0.212e in the charge for the $SrZrO_3$ and $PbZrO_3$ subsurface layers. On the Sr-terminated $SrZrO_3$ (011) surface, negative changes in the charges are observed for all atoms except for the Zr atom in the third layer (+0.039e). The largest charge changes are for the surface Sr ion (−0.087e) and especially for the subsurface O ion (−0.193e). The largest overall change in a layer charge (−0.386e) appears in the subsurface oxygen layer as well. For the O-terminated $SrZrO_3$ and $PbZrO_3$ (011) surfaces, the negative charge on the surface oxygen is very strong, and for both materials almost equally decreased (+0.094e and +0.095e). Correspondingly, the second layer becomes substantially more negative (overall change −0.025e and −0.073e). The total charge densities on the third layer (−0.005e and +0.022e) and on the central layer (+0.01e and +0.01e) are almost unchanged.

Our calculated optical band gaps corresponding to the (011) surface are considerably reduced regarding the $SrZrO_3$ and $PbZrO_3$ bulk gaps. The smallest (011) band gaps, according to our calculations are for the $SrZrO_3$ and $PbZrO_3$ Sr- and Pb-terminated (011) surfaces, 4.40 and 4.39 eV, respectively. In contrast, the optical band gap for the O-terminated $SrZrO_3$ (011) surface is only by 0.04 eV reduced with respect to the bulk value (see table 6).

Table 10. The A–B bond populations P (in e) and the relevant interatomic distances R (in Å) for three different (011) terminations in $SrZrO_3$ and $PbZrO_3$. Symbols I–IV denote the number of each plane enumerated from the surface. The nearest neighbor Zr–O distance in the unrelaxed $SrZrO_3$ bulk lattice is 2.0975 Å, and in the unrelaxed $PbZrO_3$ bulk is 2.110 Å.

$SrZrO_3$				$PbZrO_3$			
Atom A	Atom B	P	R	Atom A	Atom B	P	R
ZrO-terminated				ZrO-terminated			
Zr(I)	O(I)	0.142	2.144	Zr(I)	O(I)	0.148	2.162
	O(II)	0.246	1.933		O(II)	0.252	1.922
O(II)	Zr(III)	0.114	2.098	O(II)	Zr(III)	0.136	2.104
	Sr(III)	0.006	3.000		Pb(III)	0.030	3.030
	O(III)	0.008	3.084		O(III)	0.004	3.105
Zr(III)	Sr(III)	0.000	3.634	Zr(III)	Pb(III)	0.006	3.656
	O(III)	0.120	2.109		O(III)	0.132	2.124
	O(IV)	0.086	2.086		O(IV)	0.100	2.109
Sr(III)	O(III)	0.002	2.971	Pb(III)	O(III)	0.040	2.987
	O(IV)	0.000	2.926		O(IV)	0.040	2.935
O(III)	O(IV)	−0.036	2.854	O(III)	O(IV)	−0.044	2.872
Sr-terminated				Pb-terminated			
Sr(I)	O(II)	−0.016	2.682	Pb(I)	O(II)	0.120	2.729
O(II)	Sr(III)	+0.004	3.003	O(II)	Pb(III)	0.058	2.904
	Zr(III)	+0.080	2.132		Zr(III)	0.078	2.106
	O(III)	−0.008	3.013		O(III)	−0.062	2.924
Sr(III)	O(III)	+0.002	2.966	Pb(III)	O(III)	0.008	2.984
	O(IV)	+0.002	2.956		O(IV)	0.032	3.059
Zr(III)	O(III)	+0.058	2.098	Zr(III)	O(III)	0.056	2.113
	Sr(III)	0.000	3.633		Pb(III)	0.006	3.658
	O(IV)	+0.116	2.100		O(IV)	0.146	2.097
O(III)	O(IV)	−0.014	2.947	O(III)	O(IV)	−0.006	3.035
O-terminated				O-terminated			
O(I)	Sr(II)	+0.002	2.795	O(I)	Pb(II)	+0.066	2.847
	Zr(II)	+0.154	1.851		Zr(II)	+0.198	1.871
	O(II)	+0.016	3.051		O(II)	+0.014	3.070
Sr(II)	O(II)	−0.020	2.637	Pb(II)	O(II)	+0.062	2.494
	Zr(II)	0.000	3.498		Zr(II)	+0.006	3.629
Zr(II)	O(II)	+0.102	2.162	Zr(II)	O(II)	+0.112	2.180
	O(III)	+0.144	1.977		O(III)	+0.192	1.965
O(II)	O(III)	−0.014	2.947	O(II)	O(III)	+0.008	3.219
Sr(II)	O(III)	0.000	2.898	Pb(II)	O(III)	+0.016	3.124
O(III)	O(IV)	−0.016	2.928	O(III)	O(IV)	−0.014	3.016
	Zr(IV)	+0.068	2.147		Zr(IV)	+0.100	2.155
	Sr(IV)	0.000	2.928		Pb(IV)	+0.030	2.946

Table 11. Calculated Mulliken atomic charges Q (in e) and changes in atomic charges ΔQ with respect to the bulk charges (in e) for the three $SrZrO_3$ and $PbZrO_3$ (011) surface terminations. The Mulliken atomic charges in the $SrZrO_3$ bulk are: $+2.174e$ (Zr), $-1.351e$ (O), and $+1.880e$ (Sr). For the $PbZrO_3$ bulk they are: $+2.111e$ for Zr, $-1.160e$ for O, and $+1.368e$ for Pb.

$SrZrO_3$			$PbZrO_3$		
Atom, layer	Q	ΔQ	Atom, layer	Q	ΔQ
ZrO-terminated			ZrO-terminated		
Zr(I)	+2.177	+0.003	Zr(I)	+2.185	+0.074
O(I)	−1.273	+0.078	O(I)	−1.245	−0.085
O(II)	−1.153	+0.198	O(II)	−1.054	+0.106
Sr(III)	+1.863	−0.017	Pb(III)	+1.300	−0.068
Zr(III)	+2.193	+0.019	Zr(III)	+2.162	+0.051
O(III)	−1.303	+0.048	O(III)	−1.139	+0.021
O(IV)	−1.346	+0.005	O(IV)	−1.159	+0.001
Sr-terminated			Pb-terminated		
Sr(I)	+1.793	−0.087	Pb(I)	+1.163	−0.205
O(II)	−1.544	−0.193	O(II)	−1.145	+0.015
Sr(III)	+1.877	−0.003	Pb(III)	+1.335	−0.033
Zr(III)	+2.213	+0.039	Zr(III)	+2.166	+0.055
O(III)	−1.442	−0.091	O(III)	−1.226	−0.066
O(IV)	−1.352	−0.001	O(IV)	−1.150	+0.010
O-terminated			O-terminated		
O(I)	−1.257	+0.094	O(I)	−1.065	+0.095
Sr(II)	+1.863	−0.017	Pb(II)	+1.282	−0.086
Zr(II)	+2.215	+0.041	Zr(II)	+2.180	+0.069
O(II)	−1.400	−0.049	O(II)	−1.216	−0.056
O(III)	−1.356	−0.005	O(III)	−1.138	+0.022
Sr(IV)	+1.876	−0.004	Pb(IV)	+1.342	−0.026
Zr(IV)	+2.193	+0.019	Zr(IV)	+2.139	+0.028
O(IV)	−1.356	−0.005	O(IV)	−1.152	+0.008

4. Conclusions

According to the results of our B3LYP calculations all $SrZrO_3$ and $PbZrO_3$ (001) surface upper and third layer atoms relax inwards, while outward relaxations of all atoms in the second layer, with the exception of the second layer O atom on the SrO-terminated $SrZrO_3$ (001) surface, are found at both kinds of (001) terminations and for both materials. Inward relaxation of the first and third (001) surface layers, as well as outward relaxation of the second surface layers, according also to our previous *ab initio* calculations for $SrTiO_3$, $BaTiO_3$, $PbTiO_3$, $CaTiO_3$, and $BaZrO_3$ crystals [21, 23, 24, 26], with a few exceptions, seems to be a general behavior for ABO_3 perovskites.

Our calculated surface rumplings of 6.77% for the SrO-terminated $SrZrO_3$ (001) and 3.32% for the PbO-terminated $PbZrO_3$ (001) surfaces are almost ten times larger than those of the corresponding ZrO_2-terminated $SrZrO_3$ and $PbZrO_3$ (001) surfaces. Again, this result is in line with our previous *ab initio* studies for other perovskites, such as $SrTiO_3$, $BaTiO_3$, $PbTiO_3$, $CaTiO_3$, and $BaZrO_3$, where the AO-terminated (001) surface rumpling s was considerably larger than the BO_2-terminated (001) surface rumpling [21, 23, 24, 26], and seems to be a general rule for all our calculated ABO_3 perovskites.

Turning now to the $SrZrO_3$ and $PbZrO_3$ (011) surfaces, we found that the inward relaxation of the upper layer metal atom on the ZrO-terminated $SrZrO_3$ and $PbZrO_3$ (011) surfaces (Zr displacement of 6.16% and 6.87%) is smaller than on the SrO-terminated $SrZrO_3$ (001) surface (Sr displacement of 7.63%). However, the inward relaxations by 15.73% and 15.17% of the upper layer Sr and Pb atoms on the Sr- and Pb-terminated $SrZrO_3$ and $PbZrO_3$ (011) surfaces are about twice as large as the inward relaxation of the upper layer Sr atom on the SrO-terminated $SrZrO_3$ (001) surface. In contrast to the $SrZrO_3$ and $PbZrO_3$ (001) surfaces, our calculated atomic displacements in the third plane from the surface for the $SrZrO_3$ and $PbZrO_3$ (011) surfaces are still substantial. Our calculated surface rumplings s for the ZrO-terminated $SrZrO_3$ and $PbZrO_3$ (011) surfaces are considerably larger than those of the SrO- and PbO-terminated $SrZrO_3$ and $PbZrO_3$ (001) surfaces.

As for the surface energies, we find that both the SrO-(1.13 eV/cell) and ZrO_2-terminated (1.24 eV/cell) $SrZrO_3$ (001), as well as PbO-(1.00 eV/cell) and ZrO_2-terminated (0.93 eV/cell) $PbZrO_3$ (001) surfaces are about equally

favorable and may co-exist. In contrast, we see very large differences in surface energies on the $SrZrO_3$ (011) surfaces. Note that the $SrZrO_3$ and $PbZrO_3$ (001) surface energies are always smaller than the (011) surface energies. Also for our other calculated $SrTiO_3$, $BaTiO_3$, $PbTiO_3$, $CaTiO_3$, and $BaZrO_3$ perovskites, we can conclude that all AO- and BO_2-terminated (001) surfaces are always almost equally energetically favorable, and that for all of our calculated ABO_3 perovskites, the (001) surface energies are considerably smaller than the (011) surface energies, which means that for all our calculated ABO_3 perovskites (001) surfaces are always more stable than the (011) surfaces.

Our calculated optical band gap for the $SrZrO_3$ bulk (5.31 eV) is in a perfect agreement with the experimental value of 5.6 eV [45]. The calculated optical band gaps near the $SrZrO_3$ and $PbZrO_3$ (001) and (011) surfaces are considerably reduced with respect to the bulk band gap. This finding is in line with the narrowing of the band gap at $SrTiO_3$ and $BaTiO_3$ (001) surfaces reported earlier by Padilla and Vanderbilt [48, 49].

Our B3LYP calculations indicate a considerable increase of Zr–O chemical bond covalency near the $SrZrO_3$ and $PbZrO_3$ (011) surfaces relative to $SrZrO_3$ and $PbZrO_3$ bulk, much larger than for the (001) surface. According to our previous *ab initio* calculations, we can conclude that increase of the Ti–O (Zr–O) chemical bond covalency near the (011) surface relative to the (001) surface and bulk is a general rule also for other ABO_3 perovskites, such as $SrTiO_3$, $BaTiO_3$, $PbTiO_3$, $CaTiO_3$, and $BaZrO_3$.

Acknowledgment

The present work was supported by ESF Grant No. 2009/0202/1DP/1.1.1.2.0/09/APIA/VIAA/141.

References

[1] Matsuda T, Yamanaka S, Kurosaki K and Kobayashi S 2003 *J. Alloys Compounds* **351** 43
[2] Sengupta S S, Roberts D, Li J, Kim M C and Payne D A 1995 *J. Appl. Phys.* **78** 1171
[3] Xu B, Moses P, Pai N G and Cross L E 1998 *Appl. Phys. Lett.* **72** 593
[4] Xu B, Ye Y and Cross L E 2000 *J. Appl. Phys.* **87** 2507
[5] Pintilie L, Boldyreva K, Alexe M and Hesse D 2008 *J. Appl. Phys.* **103** 024101
[6] Wang Y X and Arai M 2007 *Surf. Sci.* **601** 4092
[7] Evarestov R A, Bandura A V and Aleksandrov V E 2007 *Surf. Sci.* **601** 1844
[8] Pilania G, Tan D Q, Cao Y, Venkataramani V S, Chen Q and Ramprasad R 2009 *J. Mater. Sci.* **44** 5249
[9] Wang Y X 2007 *Phys. Status Solidi* b **244** 602
[10] Wang Y X, Arai M, Sasaki T, Wang C L and Zhong W L 2005 *Surf. Sci.* **585** 75
[11] Bando H, Aiura Y, Haruyama Y, Shimizu T and Nishihara Y 1995 *J. Vac. Sci. Technol.* B **13** 1150
[12] Szot K and Speier W 1999 *Phys. Rev.* B **60** 5909
[13] Brunen J and Zegenhagen J 1997 *Surf. Sci.* **389** 349
[14] Jiang Q D and Zegenhagen J 1999 *Surf. Sci.* **425** 343
[15] Zegenhagen J, Haage T and Jiang Q D 1998 *Appl. Phys.* A **67** 711
[16] Souda R 1999 *Phys. Rev.* B **60** 6068
[17] Adachi Y, Kohiki S, Wagatsuma K and Oku M 1998 *J. Appl. Phys.* **84** 2123
[18] Bottin F, Finocchi F and Noguera C 2003 *Phys. Rev.* B **68** 035418
[19] Heifets E, Goddard W A, Kotomin E A, Eglitis R I and Borstel G 2004 *Phys. Rev.* B **69** 035408
[20] Asthagiri A and Sholl D 2005 *Surf. Sci.* **581** 66
[21] Eglitis R I and Vanderbilt D 2008 *Phys. Rev.* B **77** 195408
[22] Heifets E, Ho J and Merinov B 2007 *Phys. Rev.* B **75** 155431
[23] Eglitis R I 2007 *J. Phys.: Condens. Matter* **19** 356004
[24] Eglitis R I and Vanderbilt D 2007 *Phys. Rev.* B **76** 155439
[25] Zhang J M, Cui J, Xu K W, Ji V and Man Z Y 2007 *Phys. Rev.* B **76** 115426
[26] Eglitis R I and Vanderbilt D 2008 *Phys. Rev.* B **78** 155420
[27] Kennedy B J, Howard C J and Chakoumakos B C 1999 *Phys. Rev.* B **59** 4023
[28] Saunders V R, Dovesi R, Roetti C, Causa M, Harrison N M, Orlando R and Zicovich-Wilson C M 2003 *CRYSTAL-2003 User Manual* University of Torino, Torino, Italy
[29] Piskunov S, Heifets E, Eglitis R I and Borstel G 2004 *Comput. Mater. Sci.* **29** 165
[30] Heifets E, Eglitis R I, Kotomin E A, Maier J and Borstel G 2002 *Surf. Sci.* **513** 211
[31] Heifets E, Eglitis R I, Kotomin E A, Maier J and Borstel G 2001 *Phys. Rev.* B **64** 235417
[32] Becke A D 1993 *J. Chem. Phys.* **98** 5648
[33] Lee C, Yang W and Parr R G 1988 *Phys. Rev.* B **37** 785
[34] Hay P J and Wadt W R 1985 *J. Chem. Phys.* **82** 270
Hay P J and Wadt W R 1984 *J. Chem. Phys.* **82** 284
Hay P J and Wadt W R 1984 *J. Chem. Phys.* **82** 299
[35] Monkhorst H J and Pack J D 1976 *Phys. Rev.* B **13** 5188
[36] Noguera C 2000 *J. Phys.: Condens. Matter* **12** R367
[37] Tasker P W 1979 *J. Phys. C: Solid State Phys.* **12** 4977
[38] Smith A J and Welch A J 1960 *Acta Crystallogr.* **13** 653
[39] Kuroiwa Y, Sawada A, Tanaka H, Nishibori E, Takata M and Sakata M 2002 *J. Phys. Soc. Japan* **71** 2353
[40] Catlow C R A and Stoneham A M 1983 *J. Phys. C: Solid State Phys.* **16** 4321
[41] Bochiccio R C and Reale H F 1993 *J. Phys. B: At. Mol. Opt. Phys.* **26** 4871
[42] Shi H, Eglitis R I and Borstel G 2005 *Phys. Rev.* B **72** 045109
[43] Catti M, Dovesi R, Pavese A and Saunders V R 1991 *J. Phys.: Condens. Matter* **3** 4151
[44] Verstraete M and Gonze X 2003 *Phys. Rev.* B **68** 195123
[45] Lee Y S, Lee J S, Noh T W, Byun D Y, Yoo K S, Yamaura K and Takayama-Muromachi E 2003 *Phys. Rev.* B **67** 113101
[46] Bickel N, Schmidt G, Heinz K and Muller K 1989 *Phys. Rev. Lett.* **62** 2009
[47] Hikita T, Hanada T, Kudo M and Kawai M 1993 *Surf. Sci.* **287/288** 377
[48] Padilla J and Vanderbilt D 1998 *Surf. Sci.* **418** 64
[49] Padilla J and Vanderbilt D 1997 *Phys. Rev.* B **56** 1625